ULTRACOMPACT H II REGIONS

S. Kurtz and J. Franco

Instituto de Astronomía, UNAM, México

RESUMEN

Discutimos algunos resultados observacionales recientes sobre regiones H II ultracompactas. En particular, discutimos la emisión extendida de algunas regiones H II UC y el descubrimiento de una nueva clase, denominada regiones H II "hipercompactas". Además, describimos la obtención de la estructura de densidad usando la técnica del análisis del índice espectral.

ABSTRACT

We discuss some recent observational results concerning the properties of ultracompact H II regions, in particular the presence of extended continuum emission surrounding ultracompact sources and the discovery of a new class of so-called "Hypercompact" H II regions. In addition, we discuss recent attempts to probe the density structure within UC H II regions using the technique of spectral index analysis.

Key Words: **H II REGIONS — ISM: CLOUDS — RADIO CONTINUUM: ISM — STARS: EARLY-TYPE**

1. INTRODUCTION

H II regions are a relatively well-studied class of objects that are usually classified as ultracompact, compact, and extended (or classical; e.g., Habing & Israel 1979). Ultracompact (UC) H II regions have sizes of about 0.1 pc, and are located in the inner, high-pressure, parts of molecular clouds (see Kurtz et al. 2000 for a recent review). Compact H II regions have larger sizes, 0.1–0.3 pc, lower densities, and are located in more evolved zones of the clouds. Extended H II regions have sizes of up to several parsecs and they represent the mature state of these objects. Giant and supergiant H II regions are observed in external galaxies, but they represent a conglomeration of many individual H II regions that have already photoionized a large fraction of their parental giant molecular clouds. We summarize the classes of H II regions in Table 1, and list the approximate physical parameters defining each class (see Dyson & Franco 2001 for a global review). The expansion of these objects is important for our understanding of the evolution of one classification to another, as well as the structure and fate of clouds with active star formation.

In the past three years there have been at least two quite interesting observational developments in the study of UC H II regions. One deals with small-scale structures, the other with larger, more extended structures. Both will challenge theoretical models of UC H II regions and may be fruitful areas for research in coming years. In the following, we discuss these new results and their possible implications for our understanding of the formation and evolution of H II regions.

2. HISTORICAL PERSPECTIVE

Compact H II regions were first identified as a class of objects by Mezger et al. (1967), who described them as having sizes from 0.06 to 0.4 pc and electron densities close to 10^4 cm^{-3}. Qualitatively, they were described as "small, high-density H II regions *in extended H II regions of lower electron density*" (emphasis added). These "extended" regions had sizes of order 10 pc and densities of order 10^2 cm^{-3}.

In the early 1990s about a half dozen VLA surveys were made of UC H II regions including work by Wood & Churchwell (1989), Garay et al. (1993), Kurtz, Churchwell & Wood (1994), and Miralles, Rodríguez & Scalise (1994). The Galactic Plane Surveys, summarized by Becker et al. (1994) also contributed a large number of candidate UC H II regions. In total, several hundred UC H II regions were identified. These surveys were typically made at wavelengths from 2 to 6 cm, in configurations of the VLA that provided arcsecond resolution, and were sensitive to structures up to 20–30″ in size. This was a perfectly reasonable observing strategy to use: people were looking for objects expected to be < 10″ in size and with densities $n_e \sim 10^4$ cm^{-3}, which become optically thin at about 4 cm. Nevertheless, two selection effects are evident: first, that

TABLE 1

PHYSICAL PARAMETERS OF H II REGIONS

Class of Region	Size (pc)	Density (cm^{-3})	EM (pc cm^{-6})	Ionized Mass ($M_\odot$)
Hypercompact	~ 0.003	$\gtrsim 10^6$	$\gtrsim 10^{10}$	$\sim 10^{-3}$
Ultracompact	$\lesssim 0.1$	$\gtrsim 10^4$	$\gtrsim 10^7$	$\sim 10^{-2}$
Compact	$\lesssim 0.5$	$\gtrsim 5 \times 10^3$	$\gtrsim 10^7$	~ 1
Classical	~ 10	~ 100	$\sim 10^2$	$\sim 10^5$
Giant	~ 100	~ 30	$\sim 5 \times 10^5$	10^3–10^6
Supergiant	>100	~ 10	$\sim 10^5$	10^6–10^8

only structures smaller than 20–30″ are seen; second, that the highest sensitivity is to sources with turnover frequencies at about 8 GHz ($\lambda = 4$ cm). Several groups have undertaken studies to determine the significance of these selection effects; the goal of this presentation is to overview their preliminary results.

3. UC H II REGIONS WITH EXTENDED EMISSION

The primary studies of the effect of insensitivity to large-scale structures have been made by Kurtz et al. (1999) and by Kim & Koo (1996, 2001). The former began with a random selection of 15 UC H II regions and made VLA observations sensitive to structures up to 3′ in size. In 12 (80%) of these they found extended emission, and in eight (53% of 15) they suggest (on morphological grounds) that the extended emission may have a direct physical relationship to the UC H II region. An example of such extended emission is seen in the G35.20–1.74 region, shown in Figure 1. In the latter study, Kim & Koo chose 16 regions with high single-dish to interferometric flux density ratios; they found extended emission in all 16 cases. Although their work is not appropriate for a statistical study, it is the largest dataset of UC H II regions with extended emission. Furthermore, they present radio recombination line (RRL) data that support the idea that the extended emission is directly related to the ultracompact emission. This is an important point, because the physical relationship between the extended and ultracompact emission has *not* been confirmed for the Kurtz et al. sample.

The presence of the extended continuum emission is not surprising. Indeed, the original classification of compact H II regions outlined in § 2 suggests that such emission is to be expected. What has perhaps not been fully appreciated until recently is that this extended emission may be an essential part of UC H II regions, and must be accounted for both when deriving physical parameters and applying theoretical models. One possible scenario that would give rise to both ultracompact and extended ionized gas components is density structure within molecular clouds. This idea was suggested by both Franco et al. (2000a) and by Kim & Koo (2001). The latter provide a useful schematic of the idea, which is shown in Figure 2.

4. HYPERCOMPACT H II REGIONS

The other selection effect, which gives preference to regions with emission peaks at ~ 4 cm, effectively limits existing H II region surveys to objects with emission measures less than about 10^8 pc cm^{-6}. This is because $\tau_\nu \propto \nu^{-2.1}$EM, so that regions with emission measures greater than 4×10^9 pc cm^{-6} will remain optically thick into the millimeter regime. Hence, centimeter flux densities will be significantly lower than the peak flux density of the region.

Millimeter-wave observations with the VLA, using the recently developed Q-band system, have identified a number of small, very high emission measure objects (e.g., G75.78+0.34-H_2O; see Figure 1 and Carral et al. 1997). An inspection of Table shows that these regions—which we shall refer to has "hypercompact" H II regions—are more than an order of magnitude smaller and two orders of magnitude denser than UC H II regions. This is substantially more pronounced than the difference between the compact and ultracompact classifications, so we feel fully justified in defining a new class of hypercompact (HC) regions (cf., Gaume et al. 1995).

Although a new taxonomic classification is clearly warranted, it is less clear that a fundamentally new object has been discovered. In particular, it is unclear if HC H II regions are very young UC H II regions, that are still confined to very small sizes and high densities, or if they are UC H II regions that formed in a particularly high density environ-
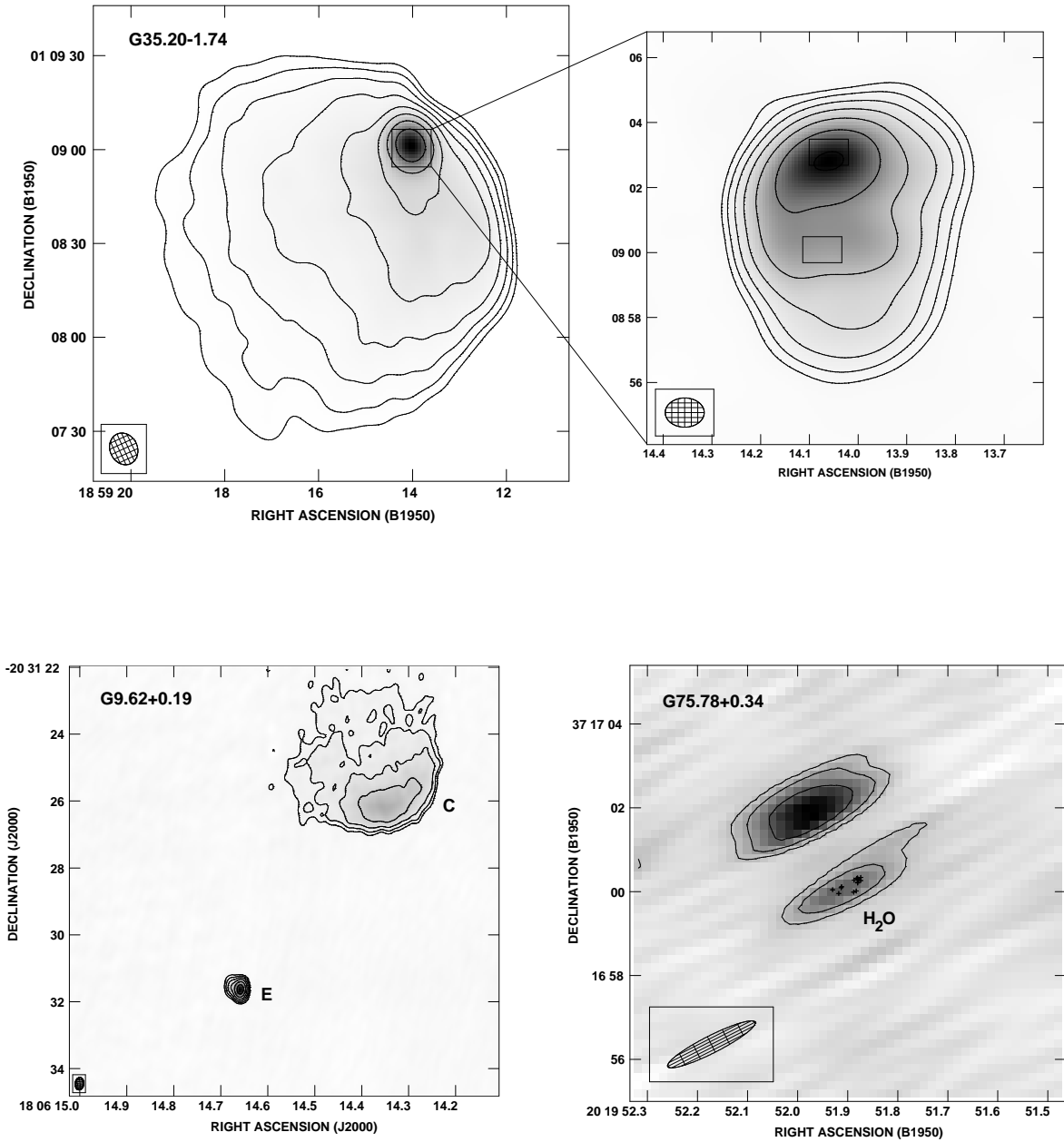
Fig. 1. This figure summarizes the essential recent developments in the study of UC H II regions. Above is shown the G35.20–1.74 UC H II region, which has a cometary morphology at at both arcsecond scales (top right) and at arcminute scales (top left). In addition, the region shows evidence for density gradients, based on a spectral index analysis of the flux densities (see figures 3 and 4). At bottom, the regions G9.62+0.19-E and G75.78+0.34-H_2O are both candidate hypercompact H II regions and both show evidence for density gradients.

ment, and which might be relatively old (see De Pree, Rodríguez & Goss 1995). A possible clue lies in the remarkable overlap between candidate HC H II regions (as indicated by very small sizes and optically thick centimeter continuum spectra) and the relatively small group of broad RRL regions (see Table 2). This overlap, first noted by Gaume (1994), suggests that HC H II regions may be in a stage of
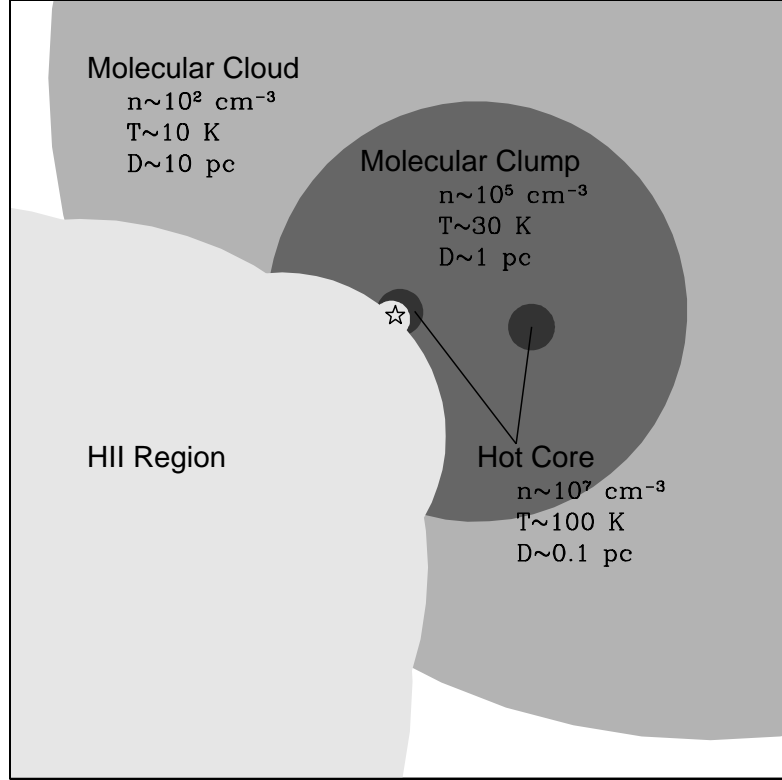
Fig. 2. Schematic representation of the model proposed by Kim & Koo to explain the extended emission around UC H II regions. The figure is not to scale; taken from Kim & Koo (2001), their Figure 8. Franco et al. (2000a) also suggest density structure within the parent molecular cloud as a possible cause of the extended emission.

rapid expansion, as would be expected for an extremely young H II region. VLA observations are underway to test this hypothesis.

5. DENSITY GRADIENTS IN H II REGIONS

For electron density distributions of power law form $n_e \propto r^{-\omega}$, the spectral index α ($S_\nu \propto \nu^\alpha$) depends on ω as $\alpha = (2\omega - 3.1)/(\omega - 0.5)$, (Olnon, 1975). Thus, multi-frequency radio observations provide a means to probe the density structure of H II regions.

Franco et al. (2000b) use this technique to study three Galactic UC H II regions (see Figure 1) and report density gradients steeper than $\omega = 1.5$. G35.20–1.74, shown at the top of Figure 1, has both compact and extended emission. The original map (inset), made with sub-arcsecond resolution, was sensitive only to structures smaller than about $20''$ (Kurtz et al. 1994) and has been convolved with a $1''2 \times 0''9$ Gaussian. The rectangular boxes indicate the integration areas used to obtain the spectral indicies reported by Franco et al. Subsequent lower resolution observations, sensitive to structures up to $3'$ in size,

show the full extent of the ionized gas in the region. Spectra for the peak and tail regions are shown in Figure 3. The need for a non-uniform density model is evident from the peak spectrum, which is reproduced in Figure 4, along with theoretical spectra corresponding to a gaussian density distribution and to a uniform distribution. The latter two dramatically under-estimate the observed flux densities.

The G9.62+0.19-E region, shown at lower left in Figure 1 in a map adapted from Testi et al. (2000), has a spectral index corresponding to a density gradient of $n_e \propto r^{-2.5}$. The spectrum of this region is shown in Figure 5, where it will also be noted that it is a candidate HC H II region. The spectrum appears to be consistent with free-free emission that remains optically thick to 2.7 mm. Alternatively, the free-free emission may be turning over at the 7 mm point, while the 2.7 mm point reflects thermal emission from warm dust.

G75.78+0.34-H$_2$O, shown at lower right in Figure 1 in a map adapted from Carral et al. (1997), has a density gradient exponent of –4, based on the
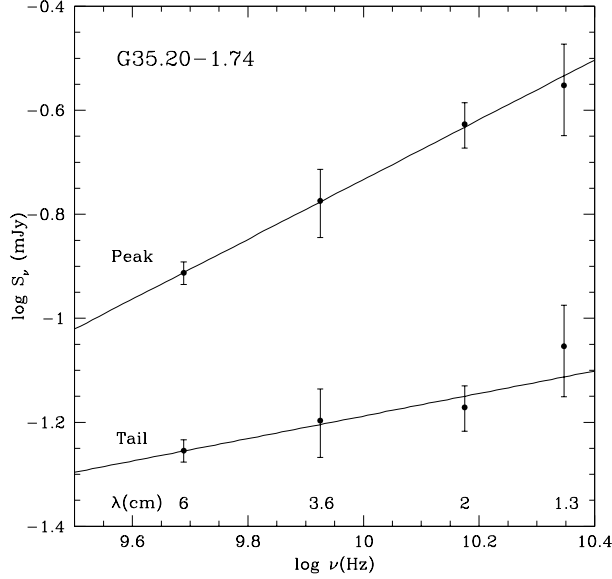
Fig. 3. The flux density distribution of G35.20−1.74. Flux densities are plotted for 4.885, 8.415, 14.965, and 22.232 GHz. The solid lines are least-squares fits, giving a spectral index at the peak position of $\alpha = 0.6 \pm 0.1$ and at the tail position of $\alpha = 0.2 \pm 0.1$. The lower spectral index in the tail region may be indicative of a transition from a steeper core gradient to a uniform inter-clump medium.

spectral index analysis of Franco et al. They suggest that a gaussian density distribution or the contribution of dust emission at high frequencies may cause this large (and probably incorrect) value.

If no mechanism acts to maintain density inhomogeneities within the H II region, they will be smoothed out on the order of a sound-crossing time (Rodríguez-Gaspar, Tenorio-Tagle & Franco 1995). This is also true for the initial density gradients, which are smoothed over time by the expansion. Thus, the density gradients that Franco et al. report are lower limits to the original distribution.

REFERENCES

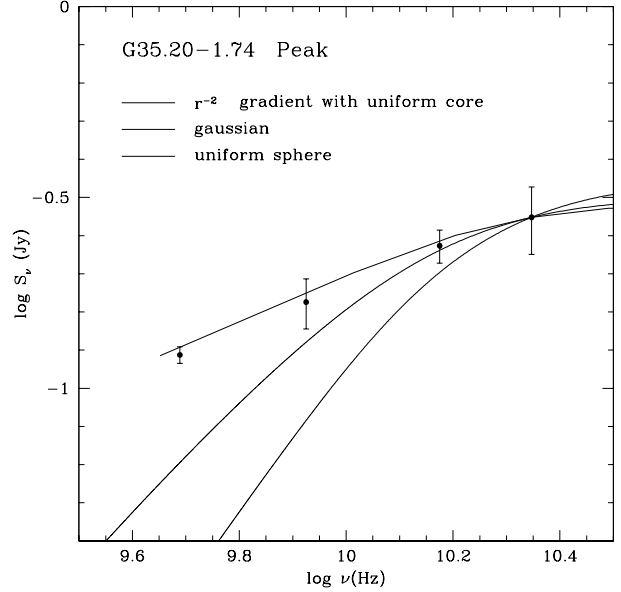Becker, R. H., White, R. L., Helfand, D. J., & Zoonematkermani, S. 1994, ApJS, 91, 347

Fig. 4. Theoretical spectra for G35.20−1.74. The data points are for the peak position, as shown in Fig. 1a. The three curves correspond to the expected flux densities for a uniform sphere of ionized gas, for a gaussian distribution, and for a flattened power law (i.e., a gradient with a uniform core). In accordance with the spectral index of the peak position, we adopt a density gradient of r^{-2}. All three curves have been scaled to match the flux density at 1.3 cm, with the assumption that this point corresponds to the turn-over frequency.

TABLE 2

KNOWN BROAD-LINE REGIONS[a]

Source	FWHM (km s^{-1})	Spectral Index	Ref
NGC 7538	180	$\cdots$	G95
G25.5+0.2	161	$\cdots$	S95
Sgr B2	80	0.95	D96
W49 AA	50	0.6	D97
W49 AB	60	1.1	D97
W49 AG	45	2	D97
M17-UC1	47	1.1	J98

REFERENCES:— G95: Gaume et al. 1995; S95: Shepherd et al. 1995; D96: De Pree et al. 1996; D97: De Pree et al. 1997; J98: Johnson et al. 1998.

[a]Table is adapted from Johnson et al. (1998).

Carral, P., Kurtz, S. E., Rodríguez, L. F., De Pree, C. G., & Hofner, P. 1997, ApJ, 486, L103

De Pree, C. G., Gaume, R. A., Goss, W. M., & Claussen, M. J. 1996, ApJ, 464, 788

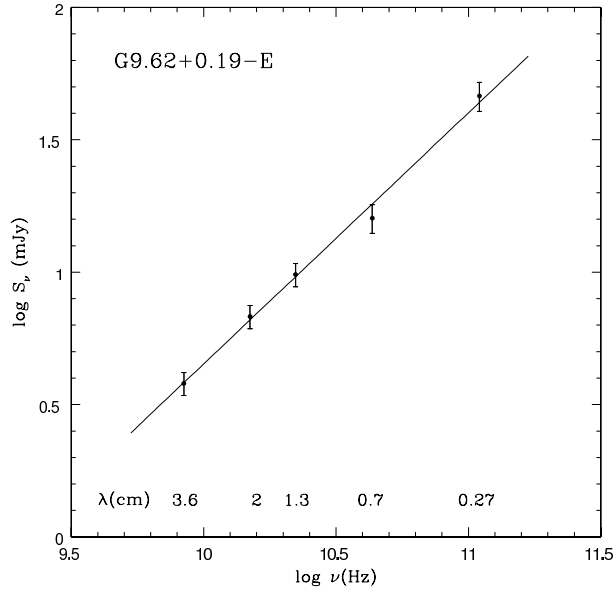De Pree, C. G., Goss, W. M., & Gaume, R. A. 1998, ApJ,

Fig. 5. The flux density distribution for G9.62+0.19-E. Flux densities are plotted for 8.415, 14.965, 22.232, 43.34, and 110 GHz. The solid line is a least-squares fit, yielding a spectral index of $\alpha = 0.95 \pm 0.06$, which suggests a density gradient of $n_e \propto r^{-2.5}$.

500, 847

De Pree, C. G., Merhinger, D. M., & Goss, W. M. 1997, ApJ, 482, 307

De Pree, C. G., Rodríguez, L. F., & Goss, W. M. 1995, RevMexAA, 31, 39

Dyson, J. E., & Franco J. 2001, in Encyclopedia of Astronomy & Astrophysics, (London: MacMillan)

Franco, J., Kurtz, S., García-Segura, G., & Hofner, P. 2000a, ApSS, 272, 169

Franco, J., Kurtz, S., Hofner, P., Testi, L., García-Segura, G., & Martos, M. 2000b, ApJ, 542, L143

Garay, G., Rodríguez, L. F., Moran, J. M., & Churchwell, E. 1993, ApJ, 418, 368

Gaume, R. A. 1994, Lecture Notes in Physics Vol. 439, eds. T. L. Wilson & K. J. Johnston (Berlin: Springer-Verlag), 199

Gaume, R. A., Goss, W. M., Dickel, H. R., Wilson, T. L., & Johnstone, K. J. 1995, ApJ, 438, 776

Habing, H. J., & Israel, F. P. 1979, ARA&A, 17, 345

Johnson, C. O., De Pree, C. G., & Goss, W. M. 1998, ApJ, 500, 302

Kim, K-T., & Koo, B-C. 1996, J. Korean Astron. Soc, 29, S177

Kim, K-T., & Koo, B-C. 2001, ApJ, 549, 979

Kurtz, S., Cesaroni, R., Churchwell, E., Hofner, P., & Walmsley, C. M. 2000, in Protostars and Planets IV, eds. Mannings, V., Boss, A. P., & Russell, S. S., (Tucson: University of Arizona Press), 299

Kurtz, S., Churchwell, E., & Wood, D. O. S. 1994, ApJS, 91, 659

Kurtz, S. E., Watson, A. M., Hofner, P. & Otte, B. 1999 ApJ, 514, 232

Mezger, P. G., Altenhoff, W., Schraml, J., Burke, B. F., Reifenstein, E. C., & Wilson, T. L. 1967, ApJ, 150, L157

Miralles, M. P., Rodríguez, L. F., & Scalise, E. 1994, ApJS, 92, 173

Olnon, F. M. 1975, A&A, 39, 217

Rodríguez-Gaspar, J. A., Tenorio-Tagle, G., & Franco, J. 1995, ApJ, 451, 210

Shepherd, D. S., Churchwell, E., & Goss, W. M., 1995, ApJ, 448, 426

Testi, L., Hofner, P., Kurtz, S., & Rupen, M. 2000, AA, 359, L5

Wood, D. O. S., & Churchwell, E. 1989, ApJS, 69, 831

S. Kurtz: Instituto de Astronomía, UNAM Campus Morelia, Apdo. Postal 3–72, 58089 Morelia, Michoacán, México (s.kurtz@astrosmo.unam.mx).

J. Franco: Instituto de Astronomía, UNAM, Apdo. Postal 70–264, 04510, México, D. F., México (pepe @astroscu.unam.mx).